JOURNAL OF AGRICULTURAL AND FOOD CHEMISTRY

Anhydrous Goat's Milk Fat: Thermal and Structural Behavior. 1. Crystalline Forms Obtained by Slow Cooling

WAFA BEN AMARA-DALI,[†,§] NADIA KARRAY,[§,‡] PIERRE LESIEUR,[#,||] AND MICHEL OLLIVON*,[†]

Equipe Physico-Chimie des Systèmes Polyphasés, UMR 8612 du CNRS, 5 rue J. B. Clément, 92296 Châtenay-Malabry, France; Unité d'Analyses Alimentaires, ENIS, BPW 3038 Sfax, Tunisia; ITPLC, Institut Technique des Produits Laitiers Caprins, Avenue F. Mitterand, BP 49, F-17700 Surgères, France; Laboratoire pour l'Utilisation du Rayonnement Electromagnétique, Orsay, France, and Lesoc, UHP-Nancy, France; and UMR 7567, Physico-Chimie des Colloïdes, Université Henri Poincaré, BP 239, 54506 Vandoeuvre-lès-Nancy, France

The thermal and structural behaviors of anhydrous goat's milk fat (AGMF) have been determined as a function of temperature using a powerful technique allowing simultaneous time-resolved synchrotron X-ray diffraction as a function of temperature (XRDT) and high-sensivity differential scanning calorimetry (DSC) measurements from the same sample. This first paper, aiming at the characterization of the physical properties of AGMF, we examine crystalline organizations made by triacylglycerols (TG) upon slow cooling at $|dT/dt| = 0.1$ °C/min from 45 to −20 °C in order to approach system equilibrium. Three overlapped exotherms were observed by DSC upon cooling, whereas four endotherms were found on the subsequent heating at 1 °C/min. XRDT evidenced that AGMF crystallizes under four different lamellar structures, two with double-chain length packings at 41.5 and 38.2 Å and two with triple-chain lengths of 72 and 64.7 Å stacking. Simultaneous wide-angle XRDT has shown that initial nucleation mainly occurs in a packing of β' type from ∼26 °C, although some transient presence of α was detected. The absence of polymorphic transition, on heating, until final melting (∼40 °C) demonstrated the relative stability of the structures formed.

KEYWORDS: Goat's milk fat; polymorphism; X-ray diffraction; differential scanning calorimetry, TG composition

INTRODUCTION

Goat's milk deserves growing interest; its milk production ranks third after cow and buffalo's milk, with an annual worldwide milk production of nearly 12.39 million metric tons in 2004 (*1*). Goat's milk and its related dairy products have a great importance in human nutrition for three reasons. First, the goat is a main supplier of dairy and meat products for rural people in the developing world, so the first use of goat's milk is home consumption. Second, goat's milk is used as a substitute for cow's milk for those who suffer from cow's milk allergy because it is widely believed to be more easily digestible (*2*−*4*). Third, goat's milk products, especially cheeses and yogurt, fill the gastronomic needs of connoisseur consumers (*4*).

Several studies have shown that the chemical composition of goat's milk, especially fat, is influenced by a number of factors including genetics factors (species, breed, and individual differences), physiological conditions (stage of lactation, age of the animal, and occurrence of mastitis), and environmental factors (especially feed composition depending on climate and season) (*5*−*8*). The anhydrous goat's milk fat (AGMF) is the fat isolated from butter. However, data about physical properties of goat's milk fat (GMF) are still scarce.

From an industrial point of view, goat's milk is directed mainly to cheese manufacture and, in a very small proportion, to other dairy products such as yogurt, butter, and milk powder. Goat's milk presents several important characteristics in butter manufacture (*6*). Fats are important components of foods providing nutritional, organoleptic, and structural properties. The milk fat of goats and cows, which is mainly composed by triacylglycerols (TG), is characterized by a broad variety of fatty acids (FA). The complexity of its composition originates from the fact that ruminants have more than one pathway for fat synthesis. This explains the extreme diversity of its FA with respect to chain lengths, position, and number of double bonds and branching.

With respective values of 2.7−6.4%, the fat content of goat's milk is higher than that of cow's milk (1.4−5.1%) (*3*, *5*, *6*, *9*, *10*). The technological and nutritional qualities of goat's milk

* Author to whom correspondence should be addressed [e-mail michel.ollivon@cep.u-psud.fr; telephone: 33-(1)-46-83-56-29; fax 33-(1)-46-83-53-12].
† Equipe Physico-Chimie des Systèmes Polyphasés.
§ Unité d'Analyses Alimentaires.
‡ ITPLC.
# Laboratoire pour l'Utilisation du Rayonnement Electromagnétique.
|| UMR 7567.

10.1021/jf051529o CCC: $30.25
Published on Web 12/01/2005

Table 1. Fatty Acid Compositions of Goat and Bovine Milk Fats According to Different Authors

fatty acid carbon no.: unsaturation position	goat (%)				bovine (%)
	a	*b*	*c*	mean	averaged range[d]
C_4:0	2.6	5.09	3.42	3.7	2–5
C_6:0	2.9	4.42	2.36	3.2	1–5
C_8:0	2.7	4.15	2.63	3.2	1–3
C_{10}:0	8.4	12.91	6.84	9.4	2–4
C_{12}:0	3.3	5.62	3.15	4	2–5
C_{14}:0	10.3	9.86	8.42	9.5	8–14
$C_{14:1\omega5}$		0.39		0.39	
C_{16}:0	24.6		23.95	24.3	22–35
$C_{16:1\omega7}$	2.2		2.10	2.15	1–3
C_{17}:0		1.26		1.3	0.5–1.5
C_{18}:0	12.5	7.17	11.58	10.4	9–14
$C_{18:1\omega9}$	28.5	15.46	25.79	23.25	20–30
$C_{18:2\omega6}$	2.2	2.83	2.89	2.65	1–3
$C_{18:3\omega3}$		0.35	1.05	0.7	0.5–2

[a] From ref *9*. [b] From ref *32*. [c] From ref *4*. [d] From ref *8*.

depend on lipids, which are the main components by weight on a dry matter basis (*6*). GMF significantly differs in average content of its fatty acids from cow's milk fat (*8*). GMF is enriched in short-chain fatty acids, from which three of their names originated, caproic ($C_{6:0}$), caprylic ($C_{8:0}$), and capric ($C_{10:0}$) acids, and in medium-chain fatty acids such as lauric ($C_{12:0}$) and sometimes myristic ($C_{14:0}$) acids. For butyric ($C_{4:0}$), palmitic ($C_{16:0}$), linoleic ($C_{18:2}$), stearic ($C_{18:0}$), and oleic ($C_{18:1}$) acids, their composition depends on many factors as said above (**Table 1**). The predominantly short-chain FAs such as caproic, caprylic, and capric acids impart a characteristic odor, flavor, and texture to the goat's milk butter (*8*). Goat's milk exceeds cow's milk in monounsaturated, polyunsaturated fatty acids and medium-chain triglycerides, some of which are supposed to be beneficial for human health (*4*).

Polymorphism is the second source of complexity of milk fat physical properties. As observed for most of the lipids, each TG of AGMF likely exhibits several crystalline forms (*11*). This polymorphism being mainly monotropic, rapidly crystallized forms are metastable, and the transitions between metastable and stable forms are irreversible. The occurrence of the different crystalline forms strongly depends on the thermal history of the TG. Because each polymorphic form is characterized by its own melting range, the melting behavior of anhydrous milk fat (AMF) is expected to be complex in relation to its composition. Lavigne et al. (*12*, *13*) have determined the composition and thermal and structural properties of anhydrous bovine's (ABMF) milk fat fractions using a series of techniques from gas and liquid chromatographies, differental scanning calorimetry (DSC), and synchrotron X-ray diffraction as a function of temperature (XRDT). The technological applications and textural properties of creams and AGMF-rich products will also depend on their thermal and structural properties as well as their TG compositions. The understanding of the functionality of AGMF in food products and of the rheological and textural properties of AGMF strongly depends on the thermal and structural properties of the TG. As observed for other fats, X-ray diffraction (XRD) and DSC are the best techniques to characterize, respectively, the structural and thermal properties of AGMF (*14*, *15*). Extensive descriptions of TG polymorphism based on data obtained using these techniques can be found in the literature (*11*, *16*). Briefly, XRD is an essential tool to identify the crystalline structures and polymorphism of pure TG and complex fats. Polymorphism results from the different possibilities of lateral packing of the FA chains and of longitudinal stacking of molecules in lamellae. These two levels of organization are identifiable from the short and long spacings observed by XRD at small and wide angles (SAXD and WAXD), respectively, as detailed in Small (*17*). The lateral packings of TG molecules frequently observed are denoted α, β', and β in the order of their increasing stability. They have been related to different subcells that have been described in detail (*18*). The longitudinal stackings of TG molecules frequently correspond to double or triple chain lengths (2L or 3L). The long spacings, measured by XRD at small angles, correspond to the repeat distance in the direction perpendicular to the lamellar.

DSC allows the characterization of the thermal properties of pure TG and fats. The consequence of the complex TG composition of fats is that they do not have a true melting point but a broad melting range. The complex DSC recordings result from both the broad distribution of TG composition and the polymorphism of monotropic type of the TG (*17*). Although the DSC recordings depend strongly on heating or cooling rates and on the entire thermal history of the sample, frequently they cannot be interpreted because of overlapping exothermic and endothermic events (*19*). XRD complements DSC for elucidating polymorphism of pure TG and fats. The coupling of XRD as a function of temperature (XRDT) and DSC was used to characterize the structural and thermal behaviors of pure TG (*12*, *20*), fats (*12*, *15*, *20*−*24*, *26*), and dispersed systems such as natural bovine and dromedary milk fat globules (*14*, *23*, *25*, *27*, *28*).

In this paper, coupling of DSC and XRDT is applied to characterize the very specific thermal and structural properties of AGMF. This paper, which is the first of a series, aims to examine the crystalline structures formed by TG during slow cooling of AGMF and their evolution as a function of temperature during a subsequent heating.

MATERIALS AND METHODS

Samples. Goat's milk was obtained from a goat herd (Dmen breed) belonging to the Arid Region Institute (Medenine, Tunisia). Sodium azide, NaN_3, was added to milk at a concentration of 0.02% (w/v) to prevent the growth of bacteria. Cream was obtained from the goat's milk after centrifugation three times at 25 °C and 3000*g* for 20 min on a Jouan GR 20 22 centrifuge (Jouan, Saint Herblain, France). AGMF was extracted from cream using the following procedure: first, after manual churning of cream (at $T = 12-15$ °C), 10 g of butter was melted to 60 °C and centrifuged for 2 min at 3000*g*. The upper organic phase was separated and filtered at 50 °C in the presence of sulfate anhydrous sodium (Na_2SO_4) on a filter of glass wool. The dried and filtered fraction constitutes the AGMF.

DSC Measurements. Thermal behaviors of AGMF were monitored by DSC using DSC-7 (Perkin-Elmer, St Quentin en Yvelines, France) equipped with Intracooler II and running under Pyris software. AGMF samples were loaded in aluminum pans of 40 μL (pan, part B014-30021; and cover, part B014-3004) that were hermetically sealed. An empty, hermetically sealed aluminum pan was used as reference.

Calibration was made with lauric acid (melting point, 43.7 °C; ΔH_m = 35.7 kJ/mol; purity > 99.9%) so that temperature and enthalpies could be corrected (*29*). AGMF samples were heated at 70 °C during 5 min to melt all crystals and nuclei. Crystallization curves were recorded from 45 to −40 °C at different cooling rates: 0.1 and 0.3 °C/min. Then, following cooling, all of the melting curves were recorded from −40 to 60 °C at 1 °C/min.

XRDT/DSC Measurements. XRD was performed using the high flux of the synchrotron beam at LURE (Laboratoire pour l'Utilisation du Rayonnement Electromagnétique, Orsay, France). DSC was performed using Microcalix, a microcalorimeter especially designed for installation in an X-ray beam (*30*). XRDT recorded at both small and wide angles and the high-sensitivity DSC setup were installed on the

D22 bench of the DCI synchrotron. Briefly, two linear detectors allow the recording of simultaneous small-angle ($q = 0-0.45$ Å^{-1}) and wide-angle ($q = 1.1-2.1$ Å^{-1}) XRD patterns with sample to detector distances of 177 and 30 cm, respectively. Both XRDT data and DSC signals are simultaneously collected from the same sample (~25 mg) with a single computer to avoid any time or temperature shift in the data collection. The channels of the detectors are calibrated to express the XRDT data in the scattering vector q with $q = 4\pi \sin(\theta)/\lambda = 2\pi/d$, where q is in angstrom^{-1}, θ in degrees is the angle of incidence of the X-ray, λ is the wavelength, and d in angstrom is the repetition distance between two planes. The calibration of the detectors was made at wide angles with high-purity tristearin, which is characterized by short spacings of 4.59, 3.85, and 3.70 ± 0.01 Å and long spacing of 44.96 Å at room temperature (*11*) complemented at small angles with silver behenate characterized with a long spacing of 58.380 ± 0.001 Å (*31*). The calorimeter coupled to XRD is calibrated with lauric acid (*30*). The samples of AGMF to be analyzed by coupled XRDT and DSC techniques were loaded into thin glass Lindeman capillaries (GLAS Muller, Berlin, Germany) as described in ref *28*.

Each XRD pattern recorded as a function of temperature simultaneously at small and wide angles was analyzed using IGOR PRO 4.0 software (Wavemetrics). For each X-ray pattern, mathematical treatments were performed to determine position, maximum intensity, and half-width at middle height of each XRD peak according to a process using a software procedure, called "findpeak_10", written for IGOR Pro 4.0 by F. Artzner (franck.artzner@univ-rennes1.ft). The diffraction peaks are fitted with the Gaussian equation

$$Y = k_0 + k_1 \exp[-[(x - k_2)/k_3]^2]$$

where k_0 = position, k_1= maxima, k_2= center, and k_3= width.

To express both variations of line position (period) and intensity on a single figure, a new representation is proposed (see **Figures 2** and **5**). In these figures, for both SAXD and WAXD analysis, the size of the symbol is proportional to the maximum of intensity of the peak, whereas the circle center indicates period. Moreover, the DSC crystallization curve, which is recorded simultaneously, is superimposed on top of the other results. As a consequence of the use of such representation, it is easier to link thermal events to structural changes.

Statistical Analysis. All DSC recordings were recorded at least in triplicate from the same AGMF sample. The XRDT patterns, which are synchrotron beam consuming, were obtained only once. However, each frame being independent of the neighboring one, their evolution can be considered more or less as a repetition of analysis, whereas DSC recording is used to validate results.

RESULTS AND DISCUSSION

AGMF was slowly cooled from 45 to −20 °C at the rate $|dT/dt| = 0.1$ °C/min to study the formation of stable crystalline forms of AGMF TG. After crystallization, the sample was analyzed on heating at $dT/dt = 1$ °C/min from −20 to 45 °C.

1. Crystalline Forms Obtained by Slow Cooling of AGMF. *1.1. Structural Analysis.* The XRD patterns, recorded as a function of time at both small and wide angles during cooling of AGMF, are presented, versus temperature, as three-dimensional plots in **Figure 1**.

The SAXD patterns (**Figure 1A**) show the progressive development of several diffraction lines corresponding to crystallization of TG in AGMF as a function of temperature.

On cooling at 0.1 °C/min, TG crystallization of AGMF starts by the appearance, at ~30 °C, of a diffraction line at $q = 0.15$ Å^{-1} (41.5 Å). The crystalline form obtained first corresponds to a lamellar structure with a longitudinal organization of molecules in a double chain length stacking ($2L_1$). At about $T = 22$ °C, two broad diffraction lines, centered at about $q = 0.08$ and 0.17 Å^{-1} (72 and 35.3 Å), are observed. Both the simultaneous increases in intensity versus temperature of these two lines during cooling and their periods suggest that they belong to the same crystalline variety. The line at 35.3 Å ($3L_{1\,(002)}$) likely corresponds to the second order of that observed at 72 Å ($3L_{1\,(001)}$) (**Figure 1A**). This second crystalline form corresponds to a lamellar structure with a triple chain length organization (3L) of the TG molecules. This form disappears shortly after crystallization after ~10 frames.

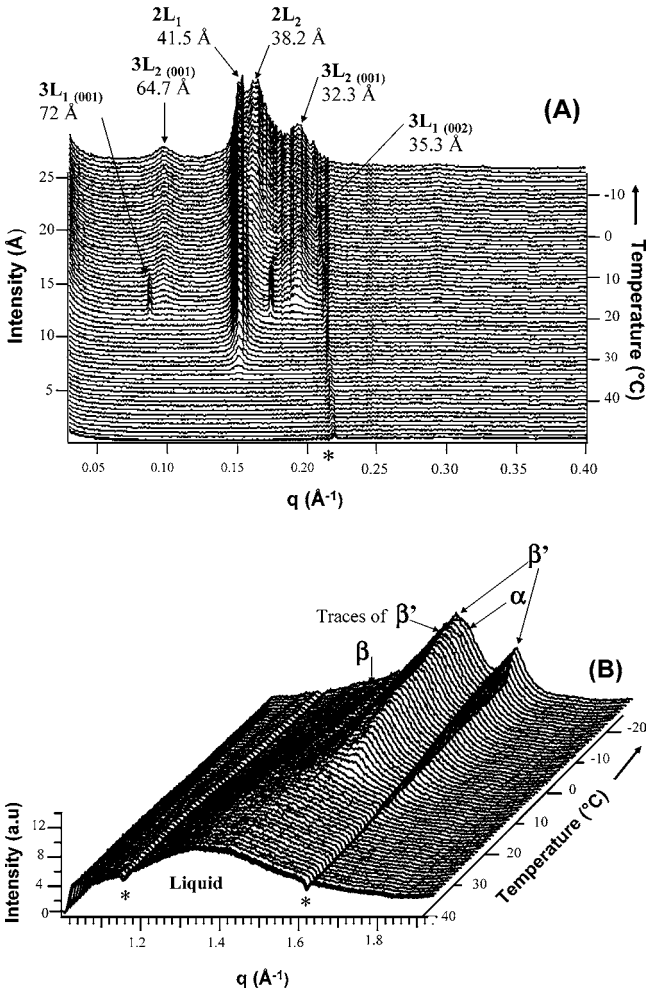

Figure 1. Three-dimensional plots of small-angle (**A**) and wide-angle (**B**) X-ray diffraction patterns recorded as a function of time during cooling of anhydrous goat's milk fat, from 45 to –20 °C, at 0.1 °C/min using coupled XRDT-DSC. (Asterisks correspond to negative peaks due to wide-angle detector defects.) The crystalline structures identified are noted in the figure.

From about 18 °C, two rather broad diffraction lines, centered at about $q = 0.09$ Å^{-1} (64.7 Å) and $q = 0.19$ Å^{-1} (32.3 Å), are observed. As above, we attributed the peaks at 64.7 and 32.3 Å to the first and second orders of a new lamellar form (**Figure 1A**). These two diffraction lines likely correspond to a new triple chain length organization [respectively ($3L_{2\,(001)}$) and ($3L_{2\,(002)}$)] of the TG molecules.

Progressively, starting from ~ 5−6 °C, a diffraction line corresponding to a 2L stacking of milk fat TG molecules is recorded at $q = 0.16$ Å^{-1} (38.1 Å). This crystalline form likely also corresponds to a lamellar structure with a double chain length ($2L_2$) of the TG molecules.

At wide angles, the recording of XRD allows identification of the lateral packing of the alkyl chains of acylglycerols in characteristic subcells. The wide-angle XRD patterns simultaneously recorded as a function of temperature (**Figure 1B**) show, at ~25 °C, the occurrence of a first diffraction line at $q = 1.64$ Å^{-1} (3.8 Å), which indicates the formation of a first crystalline

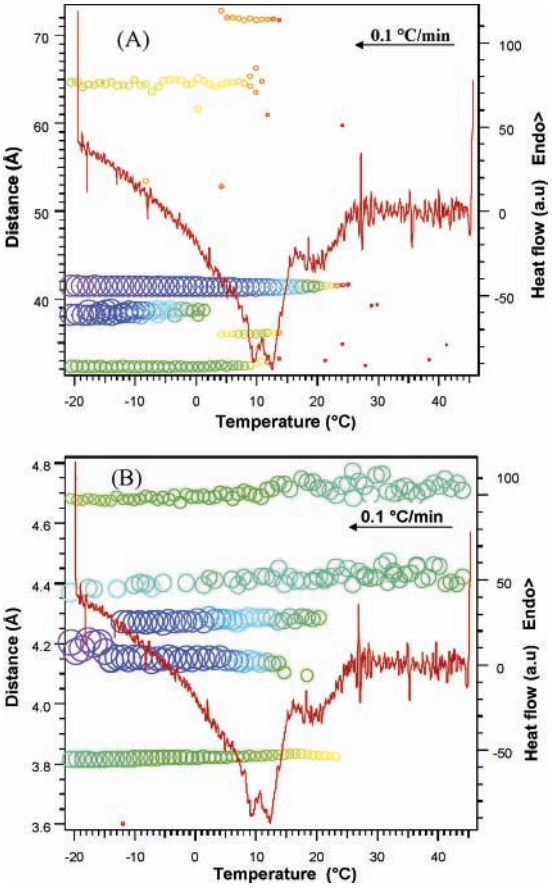

Figure 2. Evolutions, as a function of temperature of the long (**A**) and short (**B**) spacings deduced from the diffraction peaks shown in **Figure 1**, are superimposed with the DSC (raw data) crystallization curve recorded simultaneously during cooling of anhydrous goat's milk fat at 0.1 °C/min. Symbol sizes, centered on distance and temperature, are proportional to the maximum intensities of the lines.

lateral arrangement of TG chains in AGMF. Associated with a line at 4.2 Å, both lines correspond to the formation of an orthorhombic parallel packing of the chains called the β' form, which is one of the most stable possibilities of crystalline arrangement of the TG. We deduced that the occurrence of this orthorhombic packing results from the liquid to β' transition. From about 20 to −20 °C, this line increases in intensity and is accompanied by a second line at $q = 1.49$ Å^{-1} (4.2 Å). From about 18 to −20 °C, these two diffraction lines develop and are accompanied by a line at $q = 1.51$ Å^{-1} (4.1 Å) corresponding to the second organization of the lateral packing of the alkyl chains of TG in AGMF related to an hexagonal packing of the chains, called the α form.

At $T < 20$ °C, a weak line diffraction at $q = 1.34$ Å^{-1} (4.7 Å) is also observed. This line might correspond to the formation of a triclinic packing of the chains called the β form, which is also one of the two most stable forms of crystalline arrangement of the TG. The presence of traces of another β' form are observed at $q = 1.47$ Å^{-1} (4.3 Å) and at $q = 1.53$ Å^{-1} (4.1 Å). The XRD patterns recorded both at small and wide angles as a function of temperature during cooling of AGMF at $|dT/dt| = 0.1$ °C/min were analyzed using an IGOR software procedure to determine the position and the maximum intensity of each diffraction peak. The SAXD and WAXD position and intensity plots, deduced from analysis of patterns presented **Figure 1A**,**B**, are superimposed with DSC recorded simultaneously during the cooling (**Figures 2A**,**B**).

1.1.1. Spacing Evolutions. At small angles, four types of lamellar structures are observed (**Figures 1A** and **2A**). Besides the fast growth and disappearance of the 3L form (likely of α form) observed at 72 Å, the period of which apparently does not change as a function of temperature, the other 2L (41.5 and 38.2 Å) and 3L (64.7 and 32.3 Å) lamellar structures are shifting as a function of temperature (*22*). The progressive crystallization of TG as a function of the length of their FA chains likely induces the decreases of the thickness of the 2L or 3L lamellar structures formed in this range of temperature.

At wide angles, upon cooling, three to four diffraction peaks appear. They correspond to short spacings of 3.8, 4.1, 4.2, and 4.3 Å (**Figures 1B** and **2B**). The lines at about 4.3 and 4.7 Å result from software analysis of the bump corresponding to the liquid phase. The intensity of the line at 4.3 Å increases and then vanishes at lower temperature, whereas that at 4.7 Å increases with decreasing temperature, which is not shown from IGOR analysis (**Figure 2B**).

We interpreted that they are related to the formation of at least three lateral organizations of the FA chains in perpendicular orthorhombic, hexagonal, and triclinic packings. The β' phase is the major one; the β and α phases exist as only traces or intermediates, respectively. The spacing evolutions are mainly observed for 3.8 and 4.1 Å lines (**Figure 2B**). As the changes observed for long spacings they likely correspond to the progressive insertion of fatty acids with different chain lengths.

1.1.2. Evolution of Peak Intensity. The evolutions of maximum intensity of diffraction peaks recorded simultaneously at small and wide angles (**Figure 1A**,**B**) during slow cooling of AGMF are presented (**Figures 2A**,**B**) as a function of temperature (the symbol sizes are proportional to the maximum line intensities). In principle, the simultaneous recordings of small- and wide-angle XRD patterns of AGMF during cooling and the study of the variations in intensity of the lines as a function of temperature should allow relation of the lateral packings to the longitudinal organizations of TG.

At small angles, the intensity of the line 2L (41.5 Å) strongly increased from its formation at about 26 °C to about 0 °C. This strong increase, which is correlated with intensity increase of β' short spacings, should correspond to a relatively fast crystallization (**Figure 2**). The increase in intensity of the lines 3L at 72 and 35.3 Å slightly precedes that at 64.7 and 32.3 Å. As the β' type organization of acylglycerol chains with a thickness of 4.2 Å recorded at wide angles (**Figure 2B**) is the major lateral packing observed, we deduced that they are correlated. These results show that from the beginning of the crystallization process, the main lamellar crystalline variety formed in goat's milk fat corresponds to a stable β' form with a bilayered stacking. The slight increase of the line at 4.1 Å around 10 °C (**Figures 1B** and **2B**) was analyzed as temporary formation of α form. During the slow cooling of AGMF, the α form recorded at wide angles is related to the formation of the 3L structure (72 and 35.3 Å). Both wide- and small-angle α lines disappear after a few degrees of cooling, very likely because of its transformation into β'. Then, we asked ourselves to what extent the formation of β' as a major packing has favored the transition from α to β'. On the other hand, the minor β form recorded at 4.6−4.7 Å seems to be related to the formation of the 3L (38.2 Å) structure, whereas the increase of intensity of wide-angles line (**Figure 2B**) is not properly detected by IGOR analysis (see above).

1.2. Thermal Analysis. The thermal behavior of AGMF was monitored at $|dT/dt| = 0.1$ °C/min with both the coupled XRDT/DSC techniques at LURE (**Figure 2**) and the DSC-7 calorimeter

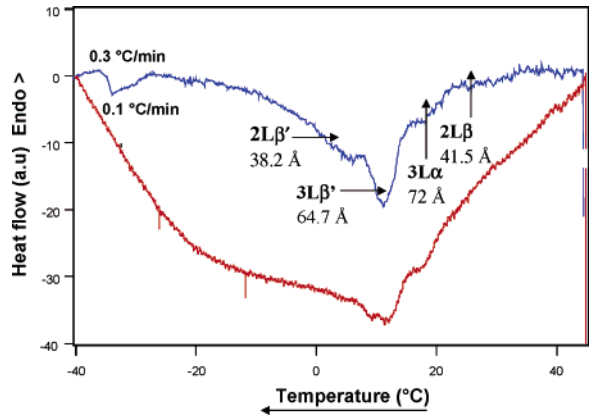

Figure 3. DSC crystallization curves recorded using DSC-7 during cooling of anhydrous goat's milk fat at 0.1 and 0.3 °C/min. Crystalline species formed during both coolings, which were deduced from XRDT analysis, are indicated. The peak observed at about −30 °C on cooling at 0.1 °C/min could not be attributed because this temperature was unattained by XRDT cooling.

(Perkin-Elmer) in the laboratory (**Figure 3**). For clarity, both panels **A** and **B** of **Figure** show the DSC recording obtained simultaneously with small- and wide-angle XRD experiments (**Figure 1A**,**B**) during cooling of AGMF. Using DSC-7, crystallization was monitored in a broader range of temperature from 45 to −40 °C against −20 °C for coupled XRDT/DSC techniques. A DSC-7 recording, which was also performed in the broad range of temperature at 0.3 °C/min in order to increase the DSC signal/noise ratio, is also presented **Figure 3**.

Comparison of structural events recorded by coupled XRDT/DSC (**Figures 1A**,**B** and **2A**,**B**) and the thermal analysis monitored by DSC-7 (**Figure 3**) allows the characterization of the crystallization behavior of AGMF. Both independent DSC recordings display an initial sharp crystallization starting at about $T \leq 26$ °C followed by several peaks with maxima at about 8 and 12 °C and spreading down to about −30 °C. All DSC crystallization curves recorded show three or four exotherms that can be correlated with the formation of the lamellar species analyzed above (**Figure 2**).

The first exothermal event recorded on cooling from ∼26 °C corresponds to the formation of the crystalline structure 2Lβ' (41.5 Å). The second and third exotherms are correlated with the formation of the lamellar 3Lα (72 Å) and 3Lβ' (64.7 Å) structures, respectively, recorded at 16 and 10 °C. The fourth exothermal event, not clearly visible in **Figure 2**, corresponds to the formation of the lamellar structure 2Lβ (38.2 Å). It is likely that at the end of the experiments recorded with coupled techniques, all of the TG are not crystallized, because the melting range of AGMF spans from about 40 to −40 °C. An exothermal peak was observed once at about −30 °C using DSC-7.

The DSC analysis presented in **Figure 3** confirms the existence of four overlapped exothermal peaks. The vanishing of the lines observed at ∼72 Å is likely associated with an endothermic process that is not easily separated from this overlapped exothermal process. Then, it cannot be ruled out that part of the sharpness of the third exotherm is due to the superimposition of a sharp endotherm.

2. Heating of AGMF after Slow Cooling. After crystallization upon cooling at $|dT/dt| = 0.1$ °C/min, the AGMF sample was heated at the rate of 1 °C/min, from −20 to 45 °C, to study the melting behavior of the supposed stable crystalline structures formed with a slow cooling rate.

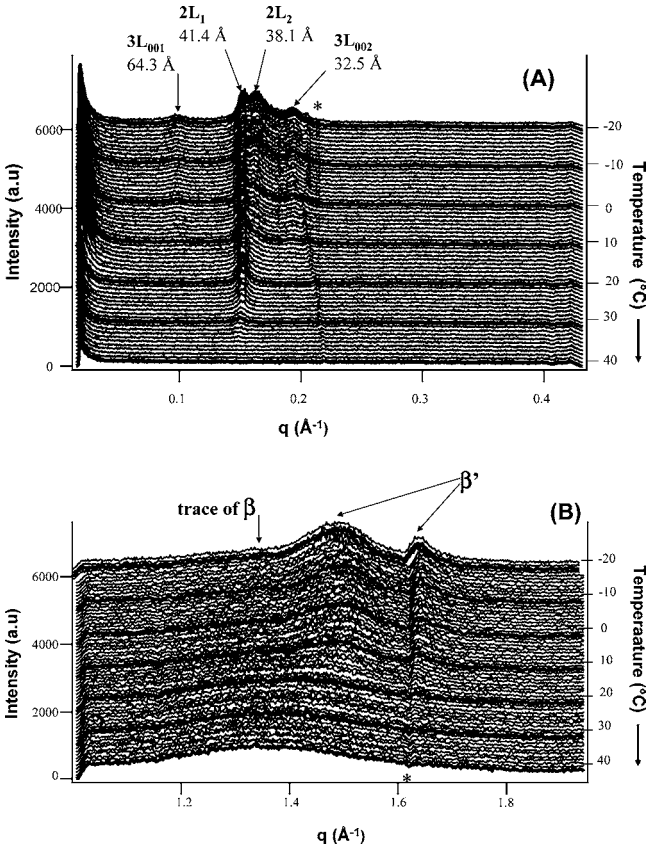

Figure 4. Three-dimensional plots of small-angle (**A**) and wide-angle (**B**) X-ray diffraction patterns recorded as a function of time during heating of anhydrous goat's milk fat at 1 °C/min after cooling at 0.1 °C/min (Asterisk as in **Figure 1**.) The crystalline structures identified are noted in the figure.

2.1.1. Structural Analysis. The XRD patterns, recorded as a function of time and T at both small and wide angles during heating of AGMF, are presented in (**Figure 4A**,**B**) as three-dimensional plots versus temperature.

The XRD patterns recorded simultaneously at small and wide angles show successively, as a function of temperature, the decrease in intensity of the diffraction lines characteristic of the 3L and 2L species. Contrary to what is observed for ABMF (*22*), no transition occurs on heating of AGMF at 1 °C/min, meaning that the crystalline species formed at 0.1 °C/min might correspond to equilibrium species.

For $T > 40$ °C, the absence of diffraction peaks at small angles and the recording of the broad peak of scattering observed at wide angles mean that all of the TG of AGMF are in their liquid state.

2.1.1. Spacing Evolution. The evolution versus temperature of the long and short spacings calculated from the peaks of diffraction recorded, respectively, at small and wide angles (**Figure 4A**,**B**) are shown in **Figure 5A**,**B**.

On heating, the long and short spacings do not show a significant evolution, meaning that no important structural reorganizations occurred and that they correspond to independent species.

However, the thickness of the 2L lamellar structure observed at 41.4 Å increases up to ∼43.5 Å at $T > 25$ °C. Again, this can be attributed to selective melting of shorter chain TG.

2.1.2. Intensity Evolution. The intensity variations of the short and long spacings recorded during heating of AGMF were plotted as a function of temperature together with DSC recordings in panels **A** and **B**, respectively, of **Figure 5** to delimit the domain ranges of existence of the crystals. Except

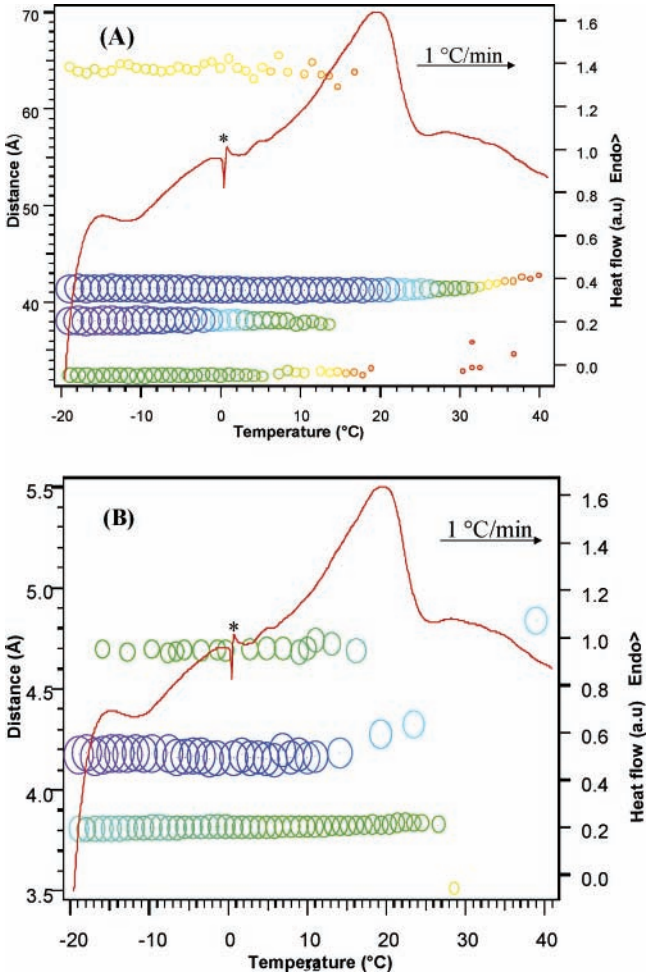

Figure 5. Evolutions, as a function of temperature of the long and short spacings deduced from the diffractions peaks, shown **Figure 4**, are superimposed with the DSC crystallization curve recorded simultaneously during heating of anhydrous goat's milk fat at 1 °C/min following its cooling at 0.1 °C/min. Symbol sizes, centered on distance and temperature, are proportional to the maximum intensities of the diffraction peaks.

for the 3Lα lines observed on cooling, the line intensity evolutions are the reverse of what is observed during the cooling process. At wide angles, the progressive vanishing of the line at 3.8 and 4.2 Å corresponds to the progressive melting of the β' organization of chains until the final melting point. The melting order is 2Lβ' (38.1 Å), 3Lβ' (64.3 Å), and 2Lβ' (41.4 Å).

2.2. Thermal Analysis. The DSC curve, recorded simultaneously with SAXD and WAXD during the heating at 1 °C/min of the AGMF sample, is presented in **Figure 5A**,**B** for clarity (the asterisk on the DSC recording indicates the melting of trace of ice in the vicinity of sample due to the duration of the slow cooling process at subzero temperatures).

The DSC melting curve shows the overlapping of several endotherms until the final melting temperature at ∼40 °C (**Figure 5**). The presence of such multiple endotherms was confirmed by DSC-7 recordings obtained in the same conditions (1 °C/min) (**Figure 6**).

The first, second, and third endotherms are recorded, respectively, in the temperature ranges of about −15 to 5, 5−22, and 22−40 °C, using both DSC-7 and DSC coupled with XRDT analysis. The absence of polymorphic evolution, on heating, as well as the high final melting point observed, ∼40 °C, confirmed that cooling at 0.1 °C/min leads to quasi equilibrium.

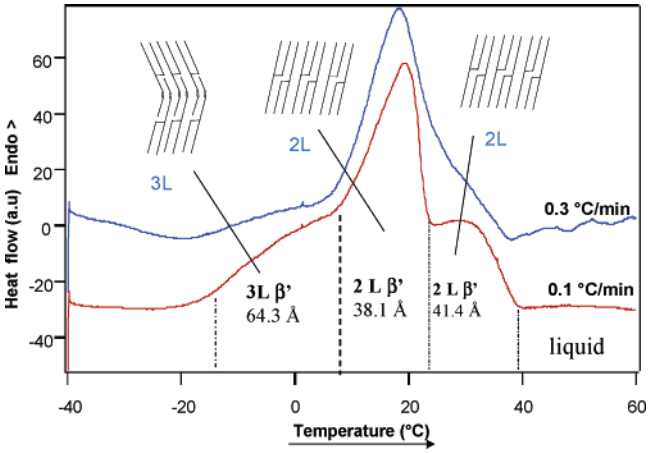

Figure 6. DSC melting curves recorded during heating at 1 °C/min of anhydrous goat's milk fat following cooling at 0.1 and 0.3 °C/min, using DSC-7 calorimeter.

Table 2. Positional Distribution of Fatty Acids on the Three Positions Glycerol of Goat and Bovine Milk Fat

	goat's milk fat[a]			cow's milk fat[b]		
fatty acid	sn-1	sn-2	sn-3	sn-1	sn-2	sn-3
C_4:0			**30.3**			**35.4**
C_6:0			**24.2**		0.9	**12.9**
C_8:0	2.3	2.2	9.2	1.4	0.7	3.6
C_{10}:0	5.0	10.5	10.2	1.9	3.0	6.2
C_{10}:1		1.65	0.5			
C_{12}:0	6.2	5.7	0.15	4.9	6.2	0.6
C_{14}:0	9.5	**21.9**	0.0	**9.7**	**17.5**	6.4
C_{14}:1	trace	0.8	1.05			
C_{15}:0	1.5	3	0.2	2.0	2.9	1.4
C_{16}:0	**41.3**	**29.5**	3.45	**34.0**	**32.3**	5.4
C_{16}:1	4.0	1.95	0.2	2.8	3.6	1.4
C_{17}:0	1.6	0.4	0.7	1.3	1.0	0.1
C_{18}:0	**11.9**	5.5	0.95	**10.3**	9.5	1.2
C_{18}:1	**14.3**	**14.2**	**13.45**	**24.0**	**30.0**	**23.1**
C_{18}:2	0.8	2.65	2.5	1.7	3.5	2.3
C_{20}:1	1.2	2.55	3.1			
C_{20}:2	0.4	0.3	0.25			

[a] From ref *33*. [b] From ref *34*.

The specific composition of AGMF deserves a tentative analysis of the DSC recordings as a function of TG melting. **Table 2** presents positional distribution of FA of goat's and bovine milk fat on glycerol as found from lipase analysis and chromatography (*33*, *34*). The esterification of the FA on glycerol results from biological processes and does not correspond to a random distribution. Although the overall FA compositions of the TG are different for both species, there are certain common features, especially for the long-chain FA.

The obvious characteristics of the FA distribution of goat's milk fat are summarized as follows: The major fatty acids in position 1 are palmitic, stearic, and oleic acids. In addition, to palmitic and stearic acids, we remark a preferential association of myristic acid with the 2-position. The main fatty acids in position 3 are butyric, caproic, and oleic acids.

From this distribution of FA at nonrandom position, we deduced the main TGs, the abbreviated names of which are reported in **Table 3**. According to the expected melting points of the different TG and polymorphic species (*17*) longitudinal and lateral packings observed, a tentative distribution of these TG into the three potential fractions (low melting point fraction, LMPF; middle melting point fraction, MMPF; and high melting point fraction, HMPF) is tentatively proposed **Table 3**. This

Table 3. Structural and Compositional Characteristics of the Fractions of AGMF and ABMF Fat during Heating at 1 °C/min[a]

endotherms	LMPF	MMPF	HMPF
melting range (°C)	−13 to −7	7−23	23−38
AGMF	3Lβ' (64.3 Å)	2Lβ' (38.1 Å)	2Lβ' (41.4 Å)
ABMF[b]	3Lα (62.2 Å)	2Lβ' (39.2 Å)	2Lβ' (41.5 Å)
		2Lβ' (48.3 Å)	
main triglycerides involved in AGMF	BuPO	PPO	PMyO
	$BuC_{10}P$	PMyO	PPO
	BuC_6P	BuPP	PPC_6
	$C_6C_6C_{10}$	Bu MyP	
	C_6PO	PPC_{10}	
		PPC_6	
		PMy C_6	
main triglycerides involved in ABMF[c]	POO	BuPP	PPP
	BuPO	PPO	PPO
	BuOO		

[a] Structural data of both fats are given as a function of the fraction determined by DSC. Main TG corresponding to the DSC profiles (tentative attribution). LMPF, low melting point fraction; MMPF, middle melting point fraction; HMPF, high melting point fraction. [b] From ref *22*. [c] From ref *12*.

analysis is based on both the analysis of milk fat fractions and the similarity of goat's and cow's milk fat DSC recordings (*13*).

The study of the thermal and structural behaviors of goat's milk fat is of great importance with regard to their economical impact and their consequences on textural and rheological properties of goat's milk-based food (especially cheese).

We believe this to be the first identification of the crystalline structures formed during a slow cooling by TG of AGMF. The lamellar organization of the TG molecules was characterized and detailed, as well as its thermal stability on heating. Coupling of small- and wide-angle time-resolved synchrotron X-ray diffraction with DSC, which allows the study of TG behavior as a function of temperature, was necessary to reveal the complex polymorphism of AGMF. Heating allowed the capture of the thermal behavior of the crystalline stable forms. The absence of structural evolution, because no polymorphic transformation is observed, during heating at 1 °C/min shows that cooling of AGMF at 0.1 °C/min leads to the formation of apparently stable species. Similar results have been found for ABMF, in previous studies, undertaken by Lavigne and Ollivon (*13*) and Lopez et al. (*22*, *23*), but further analysis demonstrated an evolution in dairy products, associated with fat polymorphism, after several days or a month. The most remarkable property of AGMF is undoubtedly its capacity to gather the ensemble of TG in three families, which generate the three melting peaks characterizing the standard AGMF DSC recording.

ABBREVIATIONS USED

AGMF, anhydrous goat's milk fat; GMF, goat's milk fat; ABMF, anhydrous bovine's milk fat; TG, triacylglycerols; DSC, differential scanning calorimetry; FA, fatty acids; 3L, trilayered stacking; 2L, bilayered stacking; SAXD, small-angle X-ray diffraction; WAXD, wide-angle X-ray diffraction; XRDT, X-ray diffraction as a function of temperature; XRD, X-ray diffraction; LMPF, low melting point fraction; MMPF, middle melting point fraction; HMPF, high melting point fraction; Bu, butyric acid; P, palmitic acid; O, oleic acid; S, stearic acid; My, myristic acid; C_6, caproic acid; C_8, caprylic acid; C_{10}, capric acid.

ACKNOWLEDGMENT

We gratefully acknowledge Prof. Hamadi Attia (ENIS, Sfax, Tunisia) for pertinent advice and drawing our interest to goat's milk fat. We thank Dr. Christelle Lopez for useful discussions and suggestions as well as Drs. Franck Artzner and Jean Blaise Brubach for assistance in the use of the IGOR software. We acknowledge T. Khorchani (Arid Region Institute, Medenine, Tunisia) for providing goat's milk. We thank ITPLC for supporting this research.

LITERATURE CITED

(1) http: //faostat.fao.org/faostat/.
(2) Aganga, A. A.; Amarteifio, J. O.; Nkile, N. Effect of Stage of Lactation on Nutrient Composition of Tswana Sheep and Goat's Milk. *J. Food Compos. Anal.* **2002**, *15*, 533−543.
(3) Haenlein, G. F. W. Past, present, and future perspectives of small ruminant dairy research. *J. Dairy Sci.* **2001**, *84*, 2097−2115.
(4) Haenlein, G. F. W. Goat milk in human nutrition. *Small Ruminant Res.* **2004**, *51*, 155−163.
(5) Guo, M.; Young, P. W.; Dixon, P. H.; Gilmore, J. A.; Kindstedt, P. S. Relationship between the yield of cheese (chevre) and chemical composition of goat milk. *Small Ruminant Res.* **2004**, *52*, 103−107.
(6) Rodriguez, A.; Bunger, A.; Castro, E.; Sousa, I.; Empis, J. Development and Optimization of cultured Goat cream butter. *J. Am. Oil Chem. Soc.* **2003**, *80*, 987−992.
(7) Jenness, R. G. The composition of Bovine Milk Lipids: January 1995 to December 2000. *J. Dairy Sci.* **2002**, *85*, 295−350.
(8) Jenness, R. G. Composition and characteristics of goat milk: review 1968−1979. *J. Dairy Sci.* **1980**, *63*, 1605−1630.
(9) Jandal, J. M. Comparative aspects of goat and sheep milk. *Small Ruminant Res.* **1996**, *22*, 177−185.
(10) Boyazoglu, J.; Morand-Fehr, P. Mediterranean dairy sheep and goat products and their quality: a critical review. *Small Ruminant Res.* **2001**, *40*, 1−11.
(11) Ollivon, M.; Perron, R. Propriétés physiques des corps gras. In *Manuel des Corps Gras*; Wolff, J. P., Karleskind, A., Guttmann, J. F., Eds.; Lavoisier: Paris, France, 1992; Vol. 1, pp 433−442.
(12) Lavigne, F. Polymorphisme et transitions de phases des triglycérides. Applications aux propriétés thermiques et structurales de la matière grasse laitière anhydre et de ses fractions; University Paris VII, Paris XI et ENSIA, 1995.
(13) Lavigne, F.; Ollivon, M. La matière grasse laitière et ses fractions. *Oléagineux, Corps Gras Lipides* **1997**, *4*, 212−219.
(14) Lopez, C.; Lesieur, P.; Keller, G.; Ollivon, M. Thermal and Structural Behavior of Milk Fat: 1. Unstable Species of Cream. *J. Colloid Interface Sci.* **2000**, *229*, 62−71.
(15) Sato, K. Polymorphism of pure triacylglycerols and natural fats. *Adv. Appl. Lipid Res.* **1996**, *2*, 213−268.
(16) Hagemann, J. W. Thermal behavior and polymorphism of acylglycerides. In *Crystallisation and Polymorphism of Fats and Fatty Acids*; Sato, K., Garti, N., Eds.; Dekker: New York, 1988; pp 9−95.
(17) Small, D. M. The physical chemistry of lipids. From alkanes to phospholipids. In *Handbook of Lipid Research*; Hanahan, D. J., Ed.; Plenum Press: New York, 1986; pp 347−382.
(18) Larsson, K. *Lipids−Molecular Organization, Physical Functions and Technical Applications*; The Oily Press: Dundee, Scotland, 1994; p 7.
(19) Appell, K, C.; Keenan, T. W.; Low, P. S. Differential scanning calorimetry of milk fat globule membranes. *Biochim. Biophys. Acta Biomembranes* **1982**, *690*, 243−250.
(20) Lopez, C.; Lesieur, P.; Bourgaux, C.; Ollivon, M. Thermal and Structural Behavior of Milk Fat. 1. Unstable Species of Anhydrous Milk Fat. *J. Dairy Sci.* **2001**, *84*, 756−766.
(21) Karrray, N.; Lopez, C.; Lesieur, P.; Ollivon, M. Dromedary milk fat: Thermal and structural properties 1−Crystalline forms obtained by slow cooling. *Lait* **2004**, *84*, 399−416.
(22) Lopez, C.; Lesieur, P.; Keller, G.; Ollivon, M. Thermal and Structural Behavior of Anhydrous Milk Fat. 2. Crystalline Forms Obtained by slow cooling. *J. Dairy Sci.* **2001**, *84*, 2402−2412.
(23) Lopez, C.; Lesieur, P.; Ollivon, M. Crystalline Structures formed in cream and anhydrous milk fat at 4 °C. *Lait* **2002**, *82*, 317−335.

(24) Lopez, C.; Lesieur, P.; Ollivon, M. Thermal and structural behavior of anhydrous milk fat: 3. Influence of cooling rate. *J. Dairy Sci.* **2005**, *88*, 511−526.
(25) Lopez, C.; Lesieur, P.; Bourgaux, C.; Keller, G.; Ollivon, M. Thermal and Structural Behavior of Milk Fat: 2. Crystalline Forms Obtained by Slow Cooling of Cream. *J. Colloid Interface Sci.* **2001**, *240*, 150−161.
(26) Karray, N.; Lopez, C.; Lesieur, P.; Ollivon, M. Dromedary milk fat: Thermal and structural properties 2—Influence of cooling rate. *Lait* **2005**, in press.
(27) Lopez, C.; Karray, N.; Lesieur, P.; Ollivon, M. Crystallisation and melting properties of dromedary milk fat globules studied by X-ray diffraction and differential scanning calorimetry. Comparison with anhydrous dromedary milk fat. *Eur. J. Lipid Sci. Technol.* **2005**, *107*, 673−683.
(28) Lopez, C.; Bourgaux, C.; Lesieur, P.; Bernadou, S.; Keller, G.; Ollivon, M. Thermal and Structural Behavior of Milk Fat: 3. Influence of Cooling Rate and Droplet Size on Cream Crystallization. *J. Colloid Interface Sci.* **2002**, *254*, 64−78.
(29) Grabielle-Madelmont, C.; Perron, R. Calorimetric Studies on Phospholipid-Water Systems. I. DL-Dipalmitoylphosphatidylcholine (DPPC)−Water System. *J. Colloid Interface Sci.* **1983**, *95*, 483−493.
(30) Keller, G.; Forte, L.; Andrieux, K.; Dahim, M.; Loisel, C.; Ollivon, M.; Bourgaux, C.; Lesieur, P. DSC and X-ray diffraction coupling. Specifications and applications. *J. Therm. Anal.* **1998**, *51*, 783−791.
(31) Blanton, T. N.; Barnes, C. L.; Lelental, M. Preparation of silver behenate coatings to provide low- to mid-angle diffraction calibration. *J. Appl. Crystallogr.* **2000**, *33*, 172−173.
(32) Fontecha, J.; Rios, J. J.; Lozada, L.; Fraga, M. J.; Juarez, M. Composition of goat's milk fat triglycerides analysed by silver ion adsorption-TLC and GC-MS. *Int. Dairy J.* **2000**, *10*, 119−128.
(33) Marai, L.; Breckenridge, W. C.; Kuksis, A. Specific distribution of fatty acids in the milk fat. Triglycerides of goat and sheep. *Lipids* **1969**, *4*, 562−570.
(34) Christie, W. W. Structures of the triacylglycerols of human milk and some substitutes. *J. Soc. Dairy Technol.* **1982**, *35*, 22−24.

Received for review June 27, 2005. Revised manuscript received October 10, 2005. Accepted October 25, 2005.

JF051529O